https://doi.org/10.5607/en22014
Exp Neurobiol. 2022 Jun;31(3):147-157.
pISSN 1226-2560 • eISSN 2093-8144

Short Communication

Experimental Neurobiology

Unaltered Tonic Inhibition in the Arcuate Nucleus of Diet-induced Obese Mice

Moonsun Sa[1,2], Jung Moo Lee[1,2], Mingu Gordon Park[1,2], Jiwoon Lim[2,3], Jong Min Joseph Kim[4], Wuhyun Koh[2], Bo-Eun Yoon[4] and C. Justin Lee[1,2,3]*

[1]KU-KIST Graduate School of Converging Science and Technology, Korea University, Seoul 02841, [2]Center for Cognition and Sociality, Institute for Basic Science (IBS), Daejeon 34126, [3]IBS School, University of Science and Technology (UST), Daejeon 34126, [4]Department of Molecular Biology, Dankook University, Cheonan 31116, Korea

The principal inhibitory transmitter, γ-aminobutyric acid (GABA), is critical for maintaining hypothalamic homeostasis and released from neurons phasically, as well as from astrocytes tonically. Although astrocytes in the arcuate nucleus (ARC) of the hypothalamus are shown to transform into reactive astrocytes, the tonic inhibition by astrocytic GABA has not been adequately investigated in diet-induced obesity (DIO). Here, we investigated the expression of monoamine oxidase- B (MAOB), a GABA-synthesizing enzyme, in reactive astrocytes in obese mice. We observed that a chronic high-fat diet (HFD) significantly increased astrocytic MAOB and cellular GABA content, along with enhanced hypertrophy of astrocytes in the ARC. Unexpectedly, we found that the level of tonic GABA was unaltered in chronic HFD mice using whole-cell patch-clamp recordings in the ARC. Furthermore, the GABA-induced current was increased with elevated $GABA_A$ receptor α5 (GABRA5) expression. Surprisingly, we found that a nonselective GABA transporter (GAT) inhibitor, nipecotic acid (NPA)-induced current was significantly increased in chronic HFD mice. We observed that GAT1 inhibitor, NO711-induced current was significantly increased, whereas GAT3 inhibitor, SNAP5114-induced current was not altered. The unexpected unaltered tonic inhibition was due to an increase of GABA clearance in the ARC by neuronal GAT1 rather than astrocytic GAT3. These results imply that increased astrocytic GABA synthesis and neuronal $GABA_A$ receptor were compensated by GABA clearance, resulting in unaltered tonic GABA inhibition in the ARC of the hypothalamus in obese mice. Taken together, GABA-related molecular pathways in the ARC dynamically regulate the tonic inhibition to maintain hypothalamic homeostasis against the HFD challenge.

Key words: Astrocyte, Arcuate nucleus, GABA transporter, High fat diet, Obesity, Tonic GABA

INTRODUCTION

The arcuate nucleus (ARC) of the hypothalamus is a part of the mediobasal hypothalamus, located near the third ventricle [1]. It is responsible for integrating information and providing inputs to other hypothalamic nuclei as well as inputs to areas outside the hypothalamus [2]. It is also home to essential and diverse neuronal populations that mediate different neuroendocrine and physiological functions [3]. The diverse functions of the ARC are dependent on its diversity of neurons, but its central role is to maintain homeostasis with respect to feeding and metabolism [4-7]. Astrocytes in the ARC participate in brain energy metabolism by controlling glycogen storage, sensing glucose, and supplying fuel to neurons under physiological conditions [8-11]. When mice are challenged by chronic high-fat diet (HFD) feeding, reactive astrocytes are observed in the ARC [12-15]. However, the pathophysiological role of reactive astrocytes in maintaining homeostasis in the ARC remains to be elucidated.

Reactive astrocytes observed under various pathological conditions have been demonstrated to acquire detrimental functions

Submitted April 17, 2022, Revised May 17, 2022,
Accepted May 18, 2022

*To whom correspondence should be addressed.
TEL: 82-42-878-9150, FAX: 82-42-878-9151
e-mail: cjl@ibs.re.kr

by tonically releasing γ-aminobutyric acid (GABA) [16-20]. The released GABA from reactive astrocytes strongly inhibits the excitability of neighboring neurons and impairs synaptic transmission and plasticity [16, 18, 19, 21]. GABA plays a fundamental role in hypothalamic homeostasis [22-24]. Synaptic GABA is synthesized by glutamic acid in neurons and is released via vesicular exocytosis, whereas non-synaptic tonic GABA is synthesized by monoamine oxidase-B (MAOB) [25] and released via bestrophin-1 channel [26]. We previously reported that reactive astrocytes in the disease state have shown a significant increase in the level of astrocytic MAOB with an increase in tonic inhibition [16, 17, 19]. Tonic inhibition, distinct from synaptic inhibition, is mediated by extrasynaptic $GABA_A$ receptors expressed in neurons [27]. The most common configuration of extrasynaptic $GABA_A$ receptors has been shown to contain either α5 (GABRA5) or δ subunit, whereas synaptic $GABA_A$ receptors have γ subunit with α1, α2 or α3, and β2/3 subunits [27-30]. The released GABA is taken up by GABA transporters (GATs) both in neurons and astrocytes [31]. GABA transporter 1 (GAT1) isoforms in neurons and GABA transporter 3 (GAT3) isoforms in astrocytes are thought to regulate ambient GABA levels in the brain [32]. Interestingly, the level of extracellular GABA was found to be elevated in the mediobasal hypothalamus, which comprises both the ventromedial hypothalamus and ARC in obese mice [33]. However, the exact extracellular ambient GABA level in the ARC has not been investigated after chronic HFD feeding. Furthermore, the source of extracellular GABA content and how chronic HFD alters extracellular $GABA_A$ receptors and GATs remain undetermined.

In this study, we hypothesized that reactive astrocytes in the ARC may play a regulatory role in maintaining homeostasis. We measured the branching of reactive astrocytes and the levels of MAOB, GABA, $GABA_A$ receptor, and GATs using immunohistochemistry. We then investigated tonic inhibition using whole-cell patch-clamp recording with drug application. We found unaltered tonic inhibition despite increased expression of MAOB and GABRA5 with elevated GAT1 in the ARC after HFD feeding. Our results propose that the increased GABA clearance compensated for the increased astrocytic GABA synthesis and neuronal $GABA_A$ receptor level, leaving the tonic inhibition unaltered.

MATERIALS AND METHODS

Animals and housing

All animal experiments were conducted according to protocols approved by the Institutional Animal Care and Use Committee of IBS (Daejeon, South Korea). All mice were maintained in a specific pathogen-free animal facility under a 12-h light-dark cycle and allowed free access to water and food. All experiments were performed on C57BL/6J background were used originated from Jackson Laboratory (USA, stock number 000664). 6-week-old male C57BL/6J mice (DBL, Chungbuk, Republic of Korea) were fed a HFD (60% kcal fat, D12492, Research Diets, USA) or chow (Teklad, 2018S, Envigo) for 20 weeks. All experiments were done with age-matched controls.

Slice preparation

Mice were anesthetized with vaporized isoflurane and then decapitated to isolate the brain. The isolated brains were excised and submerged in ice-cold NMDG recovery solution containing (in mM): 93 of NMDG, 93 of HCl, 30 of $NaHCO_3$, 20 of HEPES, 25 Glucose, 5 sodium ascorbate, 2.5 KCl, 1.2 NaH_2PO_4 (pH 7.4). All the solution was gassed with 95% O_2 and 5% CO_2. The brain was glued onto the stage of a vibrating microtome (Linear Slicer Pro7, D.S.K) and 250-μm-thick coronal slices were prepared. For stabilization, slices were incubated in room temperature for at least 1 h in extracellular aCSF solution containing (in mM): 130 of NaCl, 3.5 of KCl, 24 of $NaHCO_3$, 1.25 of NaH_2PO_4, 1.5 of $CaCl_2$, 1.5 of $MgCl_2$, and 10 of d-(+)-glucose (pH 7.4) and simultaneously equilibrated with 25℃.

Whole-cell patch-clamp recording

$GABA_A$ receptor-mediated current in the ARC was measured as previously described for tonic GABA recording [20]. Whole-cell patch-clamp recording was conducted with the holding potential of -60mV. Pipette electrode (6~8 MΩ) was filled with an internal solution (in mM): 135 of CsCl, 4 of NaCl, 0.5 of $CaCl_2$, 10 of HEPES, 5 of EGTA, 2 of Mg-ATP, 0.5 of Na_2-GTP, and 10 of QX-314, pH-adjusted to 7.2 with CsOH (278~285 mOsmol/kg). Baseline current was stabilized with D-AP5 (50 μM, 0106, Tocris, UK) and CNQX (20 μM, 0190, Tocris, UK) to isolate $GABA_A$ receptor current from NMDAR and AMPAR currents. Nipecotic acid (300 μM, 211672, Sigma-Aldrich, USA), NO711 (10 μM, N142, Sigma-Aldrich, USA), SNAP5114 (100 μM, 1561, Tocris, UK)-induced currents were recorded to isolate the contribution of neuronal GAT1 and astrocytic GAT3. Electrical signals were digitized and sampled at 10-ms intervals with Digidata 1550 B and the Multiclamp 700 B Amplifier (Molecular Devices, USA) using the pClamp10.2 software. Data were filtered at 2 kHz. Amplitude of the tonic GABA current was measured by the baseline shift in response to the bath application of bicuculline (BIC, 50 μM, 0109, Tocris, UK) using the Clampfit software (ver. 10.6.0.13.). Frequency and amplitude of spontaneous inhibitory post-synaptic currents (sIPSCs) before BIC administration was detected and measured by MiniAnalysis software (ver. 6.0.7., Synaptosoft, USA).

https://doi.org/10.5607/en22014

Immunohistochemistry

Mice were anaesthetized with isoflurane and perfused with 0.9% saline followed by ice-cold 4% paraformaldehyde (PFA). Excised brains were postfixed overnight at 4℃ and transferred to 30% sucrose for 48 hours and cut with a frozen microtome in coronal 30 μm sections. Brain sections were filled with blocking solution (0.3% Triton X-100, 3% donkey Serum in 0.1M PBS). Primary antibodies were added to blocking solution and slices were incubated in a shaker at 4℃ overnight. Primary antibodies for immunostaining were chicken anti-GFAP (1:500, AB5541, Millipore, USA), mouse anti-MAOB (1:100, sc-515354, Santa Cruz Biotechnology, USA), guinea pig anti-GABA (1:200, AB175, Millipore, USA), rabbit anti-GABRA5 (1:500, ab10098, Abcam, UK), guinea pig anti-NeuN (1:500, ABN90, Millipore, USA), rabbit anti-GAT1 (1:500, AB1570, Millipore, USA), rabbit anti-GAT3 (1:1,000, AB1574, millipore, USA). After washing, sections were incubated with corresponding secondary antibodies purchased from Jackson ImmunoResearch Laboratories (PA, USA) for 1 or 2 hours at room temperature. If needed, DAPI (1:3000, Thermo Fisher Scientific, USA) was added to PBS to visualize the nuclei of the cells. Sections were mounted with fluorescent mounting medium (S3023, Dako, Denmark) and dried. A series of fluorescent images were obtained by Zeiss LSM900 confocal microscope using a 20x, 40x objective. Z stack images were processed using the ZEN Digital Imaging for Light Microscopy blue system (Zeiss, ver. 3.2) and ImageJ (NIH, ver. 1.52s., USA) software.

Image quantification

Confocal microscopic images were analyzed in order to quantify the expression. Fluorescence intensities were calculated using the mean intensity value of each fluorescence pixels in the marker-positive area using the ImageJ (NIH, USA). Confocal images of brain sections immunostained with GFAP antibody were used for Sholl analysis. The Sholl analysis was performed on serially stacked and maximally projected confocal images and applied in Imaris software (Version 9.0.1, Oxford Instruments) constructs serially concentric circles at 10 μm intervals from the center of GFAP signal (soma) to the end of the most distal process of each astrocyte. The number of intercepts of GFAP-positive processes at each circle and the radius of the largest circle intercepting the astrocyte are analyzed.

Statistical analysis

All analysis were done blindly. The numbers and individual dots refer to the number of cells unless otherwise clarified in figure legends. The significance level is represented as asterisks (*p<0.05; **p<0.01; ***p<0.001; ****p<0.0001; n.s., not significant). Outliers were excluded by Grubb's test or ROUT method. GraphPad Prism 9.3.1 for Windows (GraphPad Software, USA) was used for these analyses and to create the plots.

RESULTS AND DISCUSSION

Elevated MAOB and GABA in reactive astrocytes after chronic HFD feeding

To measure the morphological architecture of reactive astrocytes after chronic HFD feeding, we induced mice to attain a body-weight reached 50 g (Fig. 1A, B). After 20 weeks, we performed immunostaining for GFAP, an astrocyte-specific cytoskeletal protein, and imaged it in the ARC using confocal microscopy in chow diet (Chow) and HFD mice (Fig. 1C). As reported previously [12-15], the intensity of GFAP was significantly increased in HFD mice (Fig. 1D). The morphological hypertrophy of astrocytes in the ARC of HFD mice could be clearly visualized by Sholl analysis (Fig. 1F). GFAP-positive astrocytes were significantly enhanced in the intersections as they moved radially away from soma (Fig. 1G), and the length of the ending branch and the total branch length were significantly increased in HFD mice (Fig. 1H, I). Additionally, there were significant increases in astrocytic MAOB levels (Fig. 1E) with the immunostained GABA signals in astrocytes (Fig. 1J, K). These findings indicate that chronic HFD challenge leads to a state of reactive astrocytes with increased MAOB and GABA in the ARC of the hypothalamus.

Preserved inhibitory signaling with unaltered tonic inhibition after chronic HFD feeding

To investigate whether tonic inhibition is altered in HFD mice, we measured $GABA_A$ receptor-mediated currents in the ARC after chronic HFD feeding using whole-cell patch-clamp recordings (Fig. 2A-C). The tonic current was measured by a current shift during the treatment with the $GABA_A$ receptor antagonist, bicuculline (BIC, 50 μM) in Chow mice and HFD mice (Fig. 2D). Surprisingly, the BIC-sensitive tonic inhibition current was not altered in the ARC after chronic HFD (Fig. 2F). There was also no significant difference in the amplitude and frequency of spontaneous inhibitory post-synaptic currents (sIPSCs) in Chow and HFD mice (Fig. 2E, G, H), indicating that GABAergic synaptic transmission was not changed. It has been previously shown that HFD induced oxidative stress and subsequent cellular senescence in the mouse brain [34]. In addition, dopaminergic neurons in Parkinson's disease mice exhibited decreased cell capacitance that became more severe with age [35]. To test whether chronic exposure to HFD changes the cell size, we measured the cellular capacitance, an indicator of membrane surface area. As a result, the membrane capacitance of the neurons in the ARC was significantly decreased

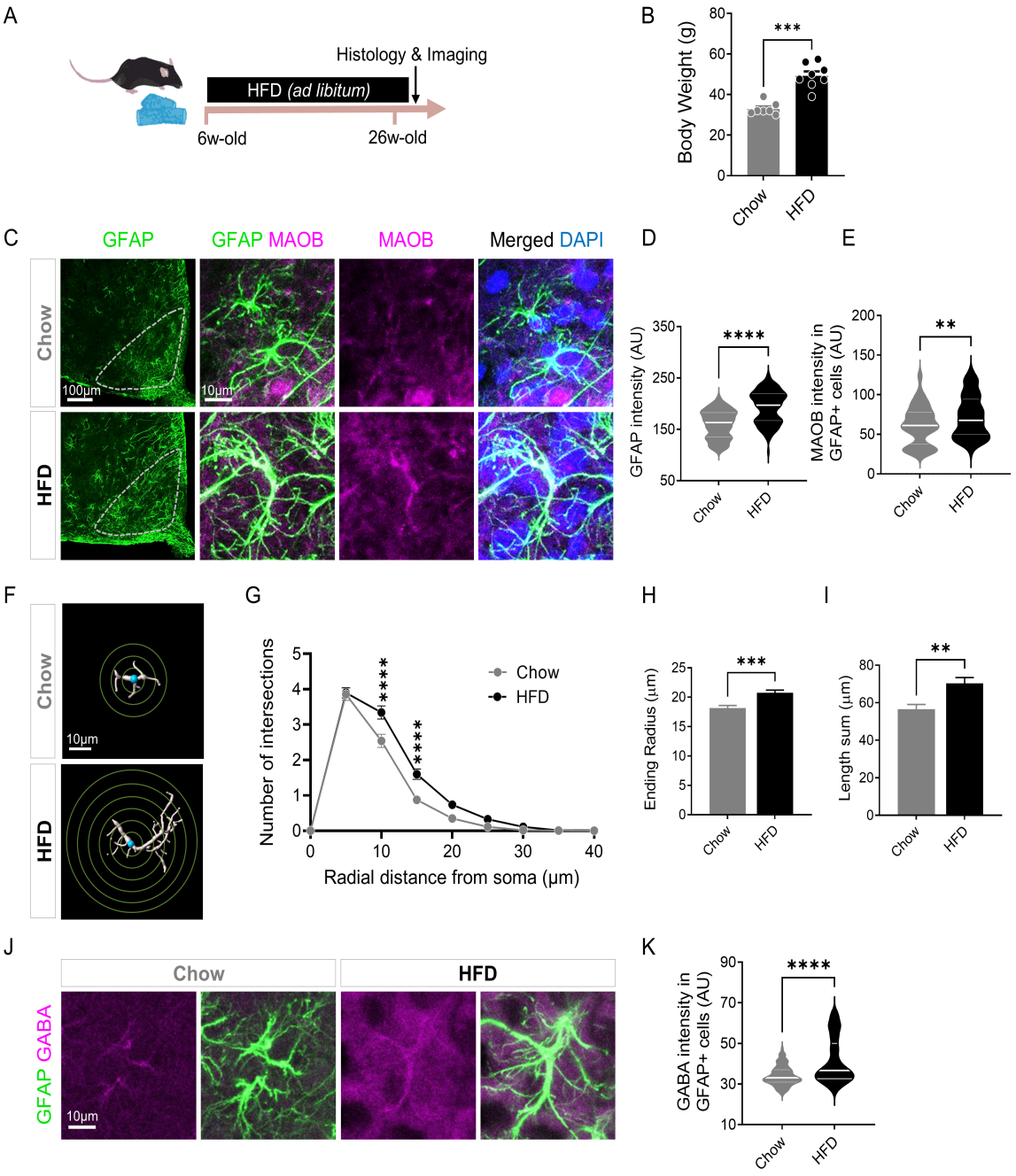

Fig. 1. Elevated MAOB and GABA in reactive astrocytes in the ARC after chronic HFD feeding. (A) Experimental timeline for high-fat diet (HFD)-induced obese mouse model. (B) Summarized bar graph showing the body weight (g) of chow diet (Chow) and HFD mice (Chow, n=7 mice; HFD, n=8 mice; Mann-Whitney test, p=0.0005). (C) Representative images of glial fibrillary acidic protein (GFAP) and monoamine oxidase B (MAOB) immunostaining in the arcuate nucleus (ARC) of Chow and HFD mice. (D) Quantification of GFAP intensity in Chow and HFD mice (Chow, n=122 cells from 3 mice; HFD, n=135 cells from 4 mice; Mann-Whitney test, p<0.0001). (E) Quantification of MAOB intensity in GFAP-positive ($GFAP^+$) cells (Chow, n=116 cells from 3 mice; HFD, n=108 cells from 4 mice; Mann-Whitney test, p=0.0069). (F) Representative images of Sholl analysis in astrocytes of Chow and HFD mice. (G) Measurement of the number of intersections according to the radial distance (μm) from the soma via Sholl analysis (Chow, n=152 cells from 3 mice; HFD, n=194 cells from 4 mice; Šťák's multiple comparisons test, p<0.0001 at 10 and 15 μm). (H) Measurement of the ending radius in Chow and HFD mice (Chow, n=152 cells; HFD, n=194 cells; Mann-Whitney test, p=0.0004). (I) Measurement of the total length in Chow and HFD mice (Chow, n=147 cells from 3 mice; HFD, n=187 cells from 4 mice; Mann-Whitney test, p=0.0050). (J) Representative images of GFAP and GABA immunostaining in the ARC of Chow and HFD mice. (K) Quantification of GABA intensity in GFAP-positive ($GFAP^+$) cells (Chow, n=106 cells from 3 mice; HFD, n=120 cells from 4 mice; Mann-Whitney test, p<0.0001). Data are presented as mean±SEM. Individual dots refer to animals. **p<0.01; ***p< 0.001; ****p<0.0001.

https://doi.org/10.5607/en22014

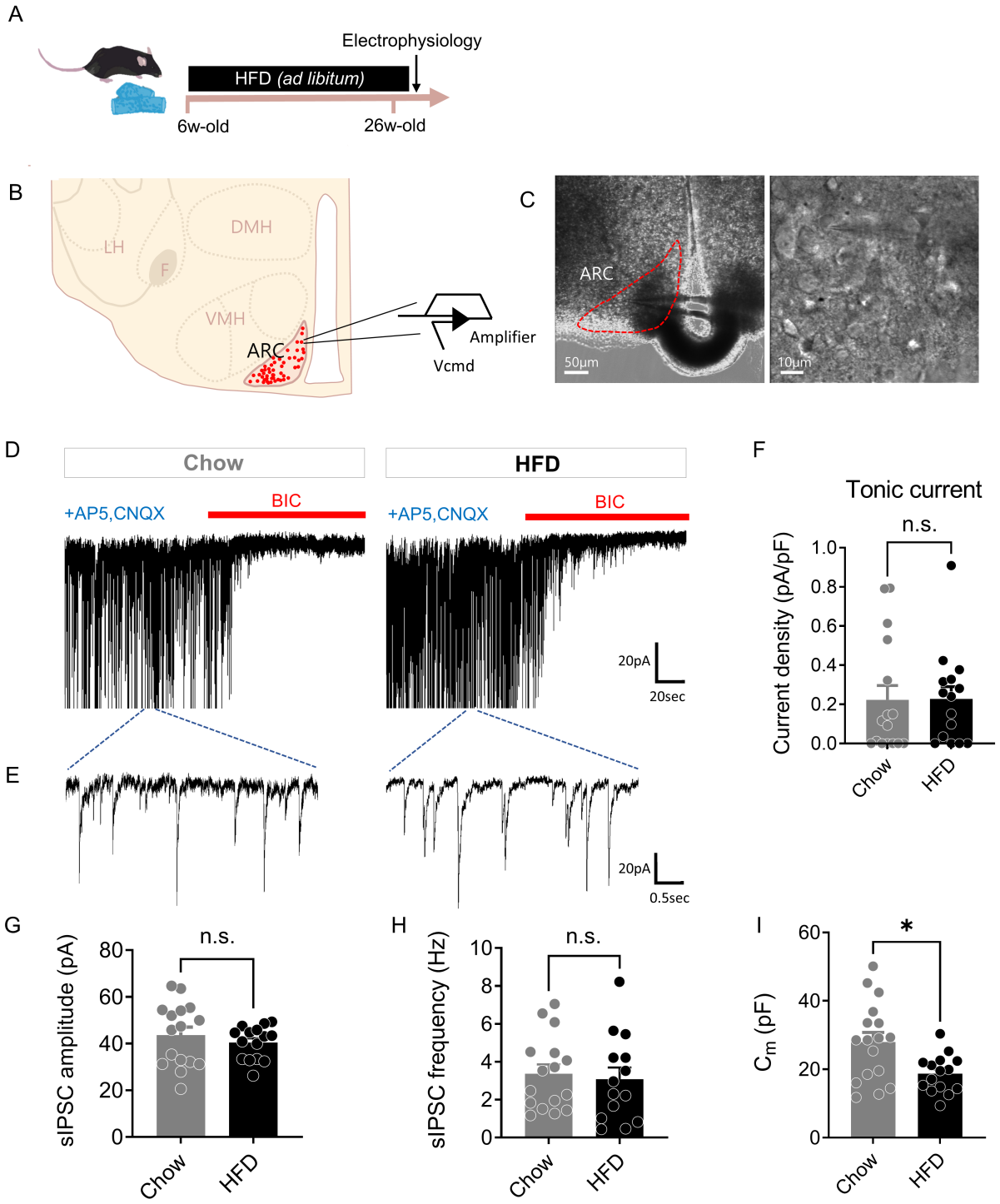

Fig. 2. Unaltered tonic inhibition in the ARC after chronic HFD feeding. (A) Experimental timeline for high-fat diet (HFD)-induced obese mouse model. (B) Schematic diagram of whole-cell patch-clamp recording in the ARC. (C) Representative infrared differential interference contrast (IR-DIC) images of whole-cell patch-clamp recording in the ARC. (D and E) Representative traces of $GABA_A$ receptor-mediated tonic GABA current (D) and spontaneous inhibitory post-synaptic current (sIPSC) (E) in Chow and HFD mice. (F) Summarized bar graph showing tonic GABA current density (pA/pF) in Chow and HFD mice (Chow, n=16 cells from 7 mice; HFD, n=15 cells from 7 mice; Mann-Whitney test, p=0.5851). (G) Summarized bar graph showing sIPSC amplitude (pA) in Chow and HFD mice (Chow, n=16 cells; HFD, n=15 cells; Mann-Whitney test, p=0.4173). (H) Summarized bar graph showing sIPSC frequency (Hz) in Chow and HFD mice (Chow, n=16 cells from 7 mice; HFD, n=14 cells from 7 mice; Mann-Whitney test, p=0.5449). (I) Summarized bar graph showing membrane capacitance (pF) in Chow and HFD mice (Chow, n=17 cells from 7 mice; HFD, n=15 cells from 7 mice; Mann-Whitney test, p=0.0238). Data are presented as mean ± SEM. *p<0.05.

in HFD mice (Fig. 2I), suggesting that chronic HFD challenges may act as toxins to neurons in the ARC and may accelerate senescence compared to age-matched Chow mice. In conclusion, both astrocytic GABA-mediated tonic inhibition and neuronal GABA-mediated phasic inhibition were not altered in chronic HFD mice.

Elevated neuronal GABRA5 in ARC after chronic HFD feeding

To test the possibility of whether chronic HFD may alter extrasynaptic $GABA_A$ receptors in the ARC, we measured the response of extrasynaptic $GABA_A$ receptors to a low concentration of GABA (10 μM) (Fig. 3A, B). We induced an inward current shift with bath application of GABA in Chow and HFD mice. We unexpectedly found that there was a significant increase in GABA-induced currents by measuring BIC-induced current shifts in the presence of GABA in the ARC of chronic HFD mice (Fig. 3C, D). Notably, a previous study reported that there was little δ subunit expression

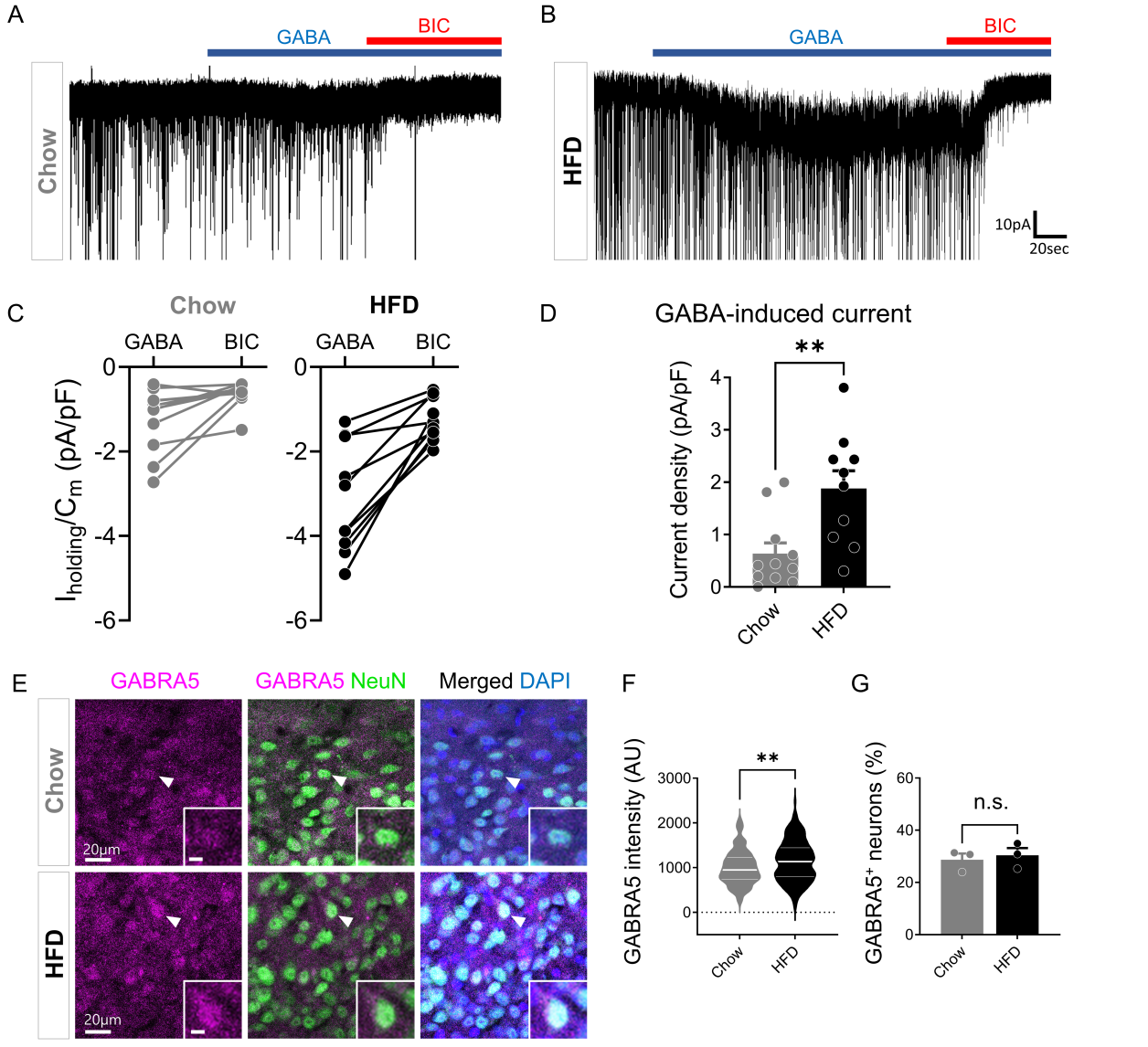

Fig. 3. Elevated extrasynaptic $GABA_A$ receptor in the ARC after chronic HFD feeding. (A and B) Representative traces of GABA-induced tonic current in Chow (A) and HFD (B) mice. (C) Paired plot showing $I_{holding}/C_m$ (pA/pF) change in Chow and HFD mice (Chow, n=11 cells from 4 mice; HFD, n=10 cells from 4 mice). (D) Summarized bar graph showing GABA-induced tonic current density (pA/pF) in chow and HFD mice (Chow, n=11 cells; HFD, n=10 cells; Mann-Whitney test, p=0.0037). (E) Representative images of GABRA5 and NeuN immunostaining in the ARC of Chow and HFD mice (inset scale bar, 5 μm). (F) Quantification of GABRA5 intensity in Chow and HFD mice (Chow, n=129 cells from 3 mice; HFD, n=208 cells from 3 mice; Mann-Whitney test, p=0.0029). (G) Percentages of GABRA5-positive neurons in Chow and HFD mice (Chow, n=3 slices from 3 mice; HFD, 3 slices from 3 mice; Mann-Whitney test, p=0.7). Data are presented as mean ± SEM. **p<0.01.

https://doi.org/10.5607/en22014

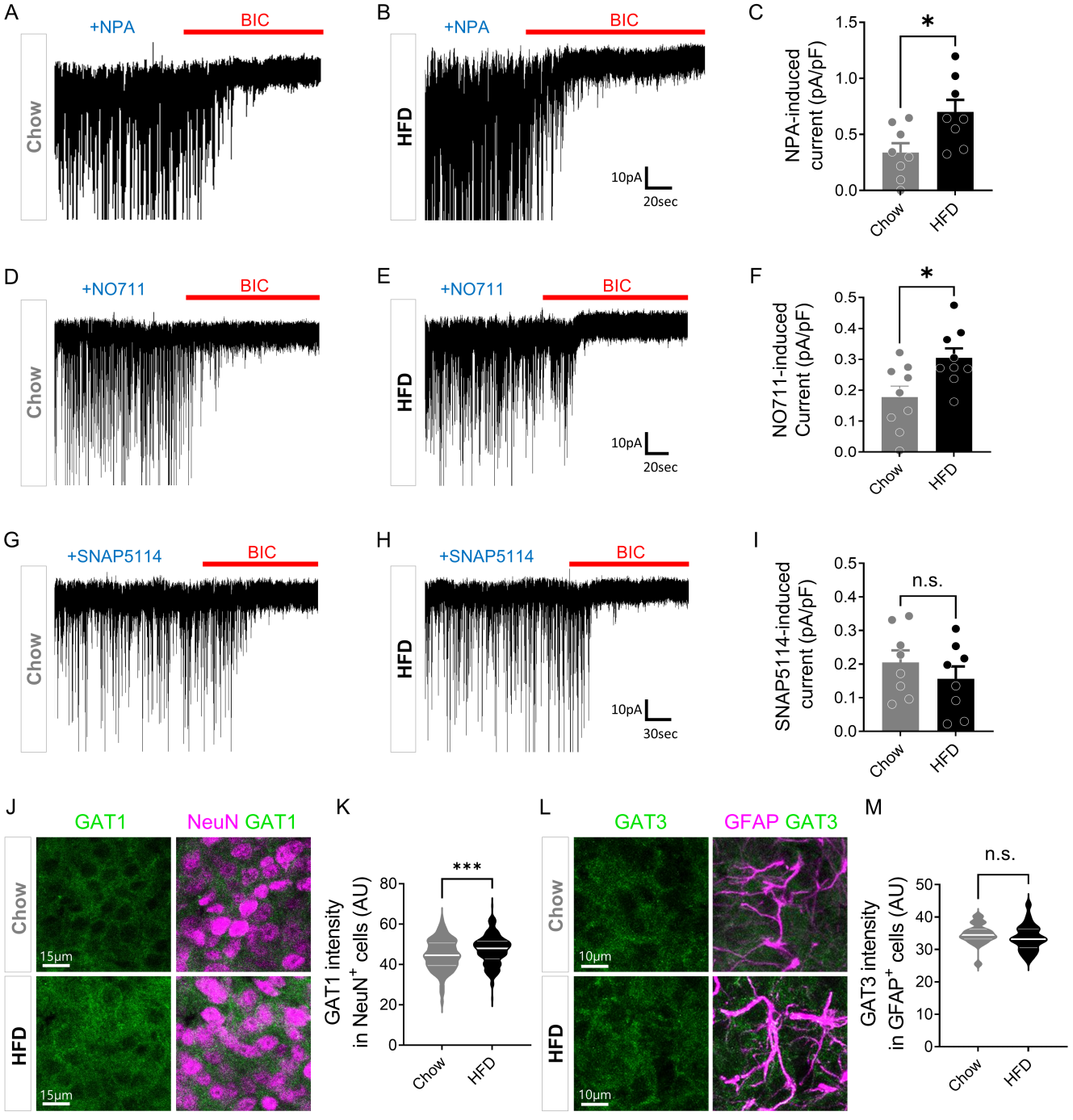

Fig. 4. Elevated neuronal GAT1, not astrocytic GAT3, in the ARC after chronic HFD feeding. (A, B) Representative traces of NPA-induced current in Chow and HFD mice. (C) Summarized bar graph showing NPA-induced current density (pA/pF) in Chow and HFD mice (Chow, n=8 cells from 3 mice; HFD, n=8 cells from 3 mice; Mann-Whitney test, p=0.0281). (D, E) Representative traces of NO711-induced current in Chow and HFD mice. (F) Summarized bar graph showing NO711-induced current density (pA/pF) in Chow and HFD mice (Chow, n=9 cells from 3 mice; HFD, n=9 cells from 3 mice; Mann-Whitney test, p=0.0315). (G, H) Representative traces of SNAP5114-induced current in Chow and HFD mice. (I) Summarized bar graph showing SNAP5114-induced current density (pA/pF) in Chow and HFD mice (Chow, n=8 cells from 2 mice; HFD, n=8 cells from 3 mice; Mann-Whitney test, p=0.3823). (J) Representative images of GAT1 and NeuN immunostaining in the ARC of Chow and HFD mice. (K) Quantification of neuronal GAT1 intensity in Chow and HFD mice (Chow, n=212 cells from 3 mice; HFD, n=300 cells from 3 mice; Mann-Whitney test, p=0.0003). (L) Representative images of GAT3 and GFAP immunostaining in the ARC of Chow and HFD mice. (M) Quantification of astrocytic GAT3 intensity in Chow and HFD mice (Chow, n=40 cells from 3 mice; HFD, n=51 cells from 3 mice; Mann-Whitney test, p=0.064). Data are presented as mean±SEM. *p<0.05; ***p<0.001.

of extrasynaptic $GABA_A$ receptor in the ARC [36]. Therefore, we investigated the expression of extrasynaptic $GABA_A$ receptor α5 subunit, previously reported to be expressed in the ARC and distinct from POMC/CART and AgRP/NPY [37]. We found that there was a significant increase in the GABRA5 expression in the ARC of chronic HFD mice using immunohistochemistry (Fig. 3E, F). However, there was no significant difference in percentages of GABRA5-positive neurons in the ARC after chronic HFD feeding (Fig. 3G). These results suggest that the increased GABA-induced full activation current is possibly due to an increased expression of GABRA5.

GAT1 compensates the enhanced tonic inhibition after chronic HFD feeding

To test the possibility that GATs may alter the tonic inhibition in chronic HFD mice, we used a non-selective GAT inhibitor, nipecotic acid (NPA, 300 μM), to inhibit GATs because GAT1 and GAT3 are sometimes considered to work synergistically in the absorption of GABA [38]. We recorded NPA-sensitive currents in the ARC of Chow and HFD mice (Fig. 4A, B). Surprisingly, NPA-induced current was significantly increased in HFD mice (Fig. 4C), indicating that GAT activity is increased after HFD. This raises the possibility that GABA uptake and clearance are enhanced in HFD mice. To investigate whether neuronal GAT1 or astrocytic GAT3 is enhanced in the ARC of HFD mice, we recorded NO711-induced currents in the ARC using a potent and selective GAT1 inhibitor [38, 39], NO711 (10 μM) (Fig. 4D, E). NO711-induced current was significantly enhanced in HFD mice (Fig. 4F). We then recorded SNAP5114-induced current using SNAP5114 (100 μM) [40] (Fig. 4G, H). However, there was no significant alteration in SNAP5114-induced current (Fig. 4I), suggesting a major role for GAT1, not GAT3 in the unaltered tonic inhibition in the ARC of HFD mice. We found that there was a significant increase in neuronal GAT1

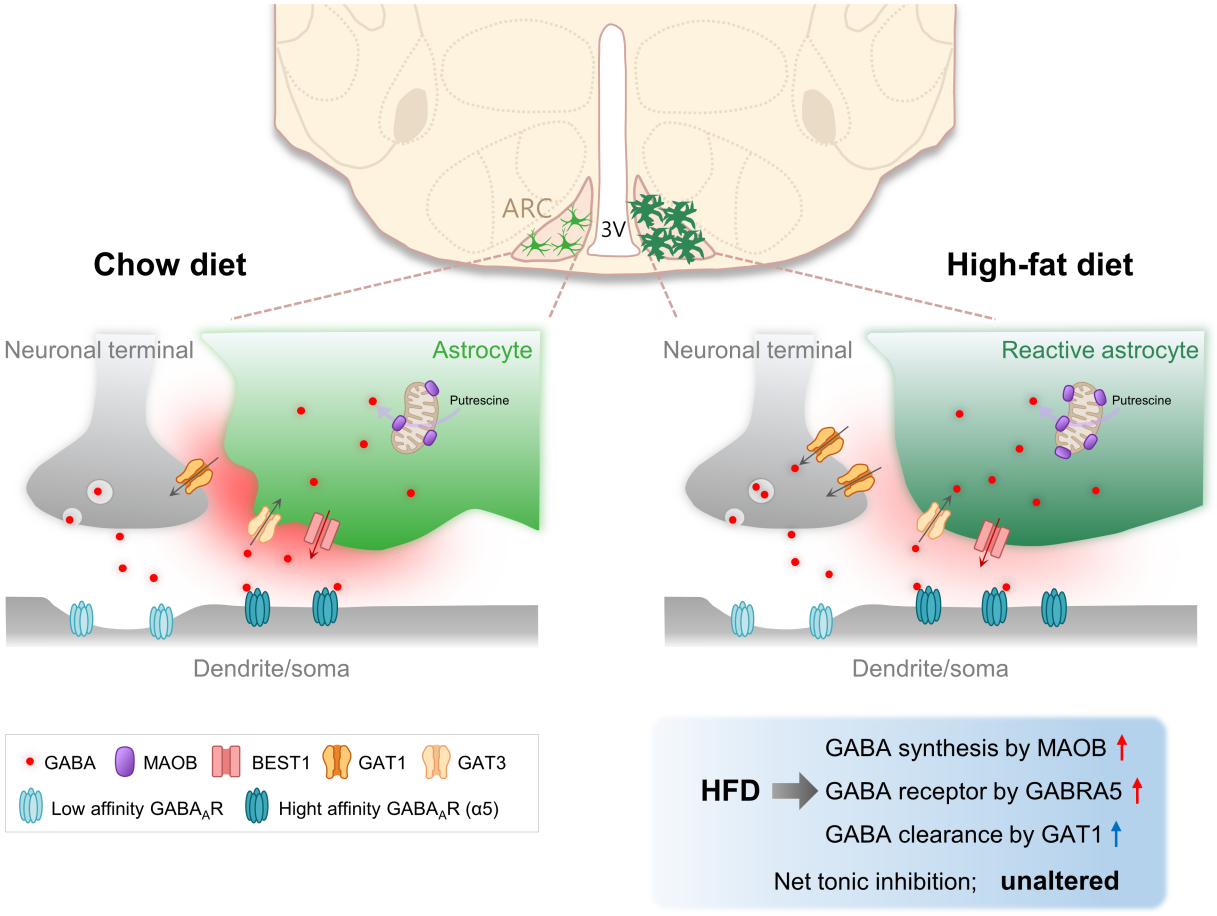

Fig. 5. Proposed working model of tonic GABA regulation in the ARC of Chow and HFD mice. In chronic high-fat diet (HFD) obese mice, astrocytes are turned into a reactive state and astrocytic GABA production is increased by monoamine oxidase-B (MAOB) in the arcuate nucleus (ARC) compared with chow diet (Chow) mice. However, tonic inhibition is not altered in HFD mice, and paradoxically, MAOB and $GABA_A$-α5 (GABRA5) expression were increased in ARC. The reason for unaltered tonic inhibition in HFD mice is that GABA transporters 1 (GAT1) compensate for the increase of GABA synthesis and $GABA_A$ receptor.

 https://doi.org/10.5607/en22014

expression (Fig. 4J, K), whereas no change in astrocytic GAT3 expression in the ARC of chronic HFD mice (Fig. 4L, M). Taken together, these findings indicate that the increased content of cellular GABA in the astrocytes and the increased neuronal $GABA_A$ receptor are compensated by the increased GAT1 activity.

In summary, we observed unaltered tonic inhibition in the ARC of HFD mice compared to chow diet mice. Chronic HFD increased astrocytic hypertrophy with an increase in GABA production via MAOB and increased extrasynaptic GABRA5. Nevertheless, unaltered tonic inhibition was attributed to an increase in GABA uptake in the ARC (Fig. 5). In our recent study, we have demonstrated that increased tonic inhibition from reactive astrocytes attenuated the firing rate of GABRA5-positive neurons in the lateral hypothalamus of HFD mice [20]. However, the tonic inhibition from reactive astrocytes was preserved in the ARC of HFD mice. These results suggest that unlike in the lateral hypothalamus, the increased GABA clearance by GAT1 compensated for the increased astrocytic GABA synthesis and neuronal $GABA_A$ receptor level, leaving the tonic inhibition unaltered in the ARC (Fig. 5).

In this study, we observed that phasic inhibition was not altered in the ARC of chronic HFD mice. However, it has been previously reported that HFD increased the excitability of AgRP neurons with an increase in the frequency and amplitude of IPSCs in AgRP neurons after 8 weeks of HFD feeding [41]. Although synaptic inhibition on AgRP neurons was significantly increased, paradoxically GABA reversal potential was depolarized by HFD [41]. This might be due to the excitatory actions of GABA [42] during the development of obesity. In 8 weeks of HFD feeding, this stage might be the process of induction of obesity, so hyperexcitability of AgRP neurons can persist despite an increase in inhibitory input. We cautiously speculate that NKCC1 expression may predominate in 8 weeks of HFD, therefore activation of $GABA_A$ receptors generates an efflux of chloride and an excitation of AgRP neurons. However, we measured IPSCs in the mice after 5 months of HFD, a time when obesity is fully established and maintained. We expect that KCC2 expression may predominate in 5 months of HFD [42]. In this stage, activation of $GABA_A$ receptors might generate an influx of chloride and an inhibition of AgRP neurons. Although we did not measure AgRP neurons specifically, the IPSCs in the ARC were not altered by HFD when obesity is established. These interesting relationships between NKCC1 predomination in the development and KCC2 predomination in the establishment of obesity await future investigation.

Our findings have not provided how tonic inhibition affects specific neuronal cell types in the ARC. Future studies are warranted to determine which specific neurons in the ARC are affected by tonic inhibition after chronic HFD feeding. We suggest that GAT1 in the ARC actively modulates inhibitory signaling by maintaining the GABA release-uptake balance in chronically established obesity. Future studies are needed to determine which neuronal cell types of GAT1 contribute to GABA clearance in the ARC. Our study is expected to provide evidence that GAT1 in the ARC could be a new molecular target for obesity.

ACKNOWLEDGEMENTS

This study was supported by the Institute for Basic Science (IBS), Center for Cognition and Sociality (IBS-R001-D2) to C.J.L.

REFERENCES

1. Daniel PM (1976) Anatomy of the hypothalamus and pituitary gland. J Clin Pathol Suppl (Assoc Clin Pathol) 7:1-7.
2. Rodríguez EM, Blázquez JL, Guerra M (2010) The design of barriers in the hypothalamus allows the median eminence and the arcuate nucleus to enjoy private milieus: the former opens to the portal blood and the latter to the cerebrospinal fluid. Peptides 31:757-776.
3. van den Top M, Spanswick D (2006) Integration of metabolic stimuli in the hypothalamic arcuate nucleus. Prog Brain Res 153:141-154.
4. Waterson MJ, Horvath TL (2015) Neuronal regulation of energy homeostasis: beyond the hypothalamus and feeding. Cell Metab 22:962-970.
5. Sohn JW (2015) Network of hypothalamic neurons that control appetite. BMB Rep 48:229-233.
6. Roh E, Kim MS (2016) Brain regulation of energy metabolism. Endocrinol Metab (Seoul) 31:519-524.
7. Rossi MA, Stuber GD (2018) Overlapping brain circuits for homeostatic and hedonic feeding. Cell Metab 27:42-56.
8. Bélanger M, Allaman I, Magistretti PJ (2011) Brain energy metabolism: focus on astrocyte-neuron metabolic cooperation. Cell Metab 14:724-738.
9. Choi HB, Gordon GR, Zhou N, Tai C, Rungta RL, Martinez J, Milner TA, Ryu JK, McLarnon JG, Tresguerres M, Levin LR, Buck J, MacVicar BA (2012) Metabolic communication between astrocytes and neurons via bicarbonate-responsive soluble adenylyl cyclase. Neuron 75:1094-1104.
10. Fuente-Martín E, García-Cáceres C, Granado M, de Ceballos ML, Sánchez-Garrido MÁ, Sarman B, Liu ZW, Dietrich MO, Tena-Sempere M, Argente-Arizón P, Díaz F, Argente J, Horvath TL, Chowen JA (2012) Leptin regulates glutamate and glucose transporters in hypothalamic astrocytes. J Clin Invest

122:3900-3913.
11. García-Cáceres C, Quarta C, Varela L, Gao Y, Gruber T, Legutko B, Jastroch M, Johansson P, Ninkovic J, Yi CX, Le Thuc O, Szigeti-Buck K, Cai W, Meyer CW, Pfluger PT, Fernandez AM, Luquet S, Woods SC, Torres-Alemán I, Kahn CR, Götz M, Horvath TL, Tschöp MH (2016) Astrocytic insulin signaling couples brain glucose uptake with nutrient availability. Cell 166:867-880.
12. Thaler JP, Yi CX, Schur EA, Guyenet SJ, Hwang BH, Dietrich MO, Zhao X, Sarruf DA, Izgur V, Maravilla KR, Nguyen HT, Fischer JD, Matsen ME, Wisse BE, Morton GJ, Horvath TL, Baskin DG, Tschöp MH, Schwartz MW (2012) Obesity is associated with hypothalamic injury in rodents and humans. J Clin Invest 122:153-162.
13. González-García I, García-Cáceres C (2021) Hypothalamic astrocytes as a specialized and responsive cell population in obesity. Int J Mol Sci 22:6176.
14. Horvath TL, Sarman B, García-Cáceres C, Enriori PJ, Sotonyi P, Shanabrough M, Borok E, Argente J, Chowen JA, Perez-Tilve D, Pfluger PT, Brönneke HS, Levin BE, Diano S, Cowley MA, Tschöp MH (2010) Synaptic input organization of the melanocortin system predicts diet-induced hypothalamic reactive gliosis and obesity. Proc Natl Acad Sci U S A 107:14875-14880.
15. Sa M, Park MG, Lee CJ (2022) Role of hypothalamic reactive astrocytes in diet-induced obesity. Mol Cells 45:65-75.
16. Jo S, Yarishkin O, Hwang YJ, Chun YE, Park M, Woo DH, Bae JY, Kim T, Lee J, Chun H, Park HJ, Lee DY, Hong J, Kim HY, Oh SJ, Park SJ, Lee H, Yoon BE, Kim Y, Jeong Y, Shim I, Bae YC, Cho J, Kowall NW, Ryu H, Hwang E, Kim D, Lee CJ (2014) GABA from reactive astrocytes impairs memory in mouse models of Alzheimer's disease. Nat Med 20:886-896.
17. Chun H, An H, Lim J, Woo J, Lee J, Ryu H, Lee CJ (2018) Astrocytic proBDNF and tonic GABA distinguish active versus reactive astrocytes in hippocampus. Exp Neurobiol 27:155-170.
18. Nam MH, Cho J, Kwon DH, Park JY, Woo J, Lee JM, Lee S, Ko HY, Won W, Kim RG, Song H, Oh SJ, Choi JW, Park KD, Park EK, Jung H, Kim HS, Lee MC, Yun M, Lee CJ, Kim HI (2020) Excessive astrocytic GABA causes cortical hypometabolism and impedes functional recovery after subcortical stroke. Cell Rep 32:107861.
19. Heo JY, Nam MH, Yoon HH, Kim J, Hwang YJ, Won W, Woo DH, Lee JA, Park HJ, Jo S, Lee MJ, Kim S, Shim JE, Jang DP, Kim KI, Huh SH, Jeong JY, Kowall NW, Lee J, Im H, Park JH, Jang BK, Park KD, Lee HJ, Shin H, Cho IJ, Hwang EM, Kim Y, Kim HY, Oh SJ, Lee SE, Paek SH, Yoon JH, Jin BK, Kweon GR, Shim I, Hwang O, Ryu H, Jeon SR, Lee CJ (2020) Aberrant tonic inhibition of dopaminergic neuronal activity causes motor symptoms in animal models of Parkinson's disease. Curr Biol 30:276-291.e9.
20. Sa M, Yoo ES, Koh W, Park MG, Jang HJ, Yang YR, Lim J, Won W, Kwon J, Bhalla M, An H, Seong Y, Lee SE, Park KD, Suh PG, Sohn JW, Lee CJ (2022) Hypothalamic GABRA5-positive neurons control obesity via astrocytic GABA. bioRxiv. doi: 10.1101/2021.11.07.467613.
21. Park JH, Ju YH, Choi JW, Song HJ, Jang BK, Woo J, Chun H, Kim HJ, Shin SJ, Yarishkin O, Jo S, Park M, Yeon SK, Kim S, Kim J, Nam MH, Londhe AM, Kim J, Cho SJ, Cho S, Lee C, Hwang SY, Kim SW, Oh SJ, Cho J, Pae AN, Lee CJ, Park KD (2019) Newly developed reversible MAO-B inhibitor circumvents the shortcomings of irreversible inhibitors in Alzheimer's disease. Sci Adv 5:eaav0316.
22. Delgado TC (2013) Glutamate and GABA in appetite regulation. Front Endocrinol (Lausanne) 4:103.
23. Tong Q, Ye CP, Jones JE, Elmquist JK, Lowell BB (2008) Synaptic release of GABA by AgRP neurons is required for normal regulation of energy balance. Nat Neurosci 11:998-1000.
24. Wu Q, Boyle MP, Palmiter RD (2009) Loss of GABAergic signaling by AgRP neurons to the parabrachial nucleus leads to starvation. Cell 137:1225-1234.
25. Yoon BE, Woo J, Chun YE, Chun H, Jo S, Bae JY, An H, Min JO, Oh SJ, Han KS, Kim HY, Kim T, Kim YS, Bae YC, Lee CJ (2014) Glial GABA, synthesized by monoamine oxidase B, mediates tonic inhibition. J Physiol 592:4951-4968.
26. Lee S, Yoon BE, Berglund K, Oh SJ, Park H, Shin HS, Augustine GJ, Lee CJ (2010) Channel-mediated tonic GABA release from glia. Science 330:790-796.
27. Farrant M, Nusser Z (2005) Variations on an inhibitory theme: phasic and tonic activation of GABA(A) receptors. Nat Rev Neurosci 6:215-229.
28. Brickley SG, Cull-Candy SG, Farrant M (1996) Development of a tonic form of synaptic inhibition in rat cerebellar granule cells resulting from persistent activation of GABAA receptors. J Physiol 497(Pt 3):753-759.
29. Stell BM, Mody I (2002) Receptors with different affinities mediate phasic and tonic GABA(A) conductances in hippocampal neurons. J Neurosci 22:RC223.
30. Nusser Z, Mody I (2002) Selective modulation of tonic and phasic inhibitions in dentate gyrus granule cells. J Neurophysiol 87:2624-2628.
31. Scimemi A (2014) Structure, function, and plasticity of GABA transporters. Front Cell Neurosci 8:161.
32. Dalby NO (2003) Inhibition of gamma-aminobutyric acid

uptake: anatomy, physiology and effects against epileptic seizures. Eur J Pharmacol 479:127-137.
33. Zhang Y, Reichel JM, Han C, Zuniga-Hertz JP, Cai D (2017) Astrocytic process plasticity and IKKβ/NF-κB in central control of blood glucose, blood pressure, and body weight. Cell Metab 25:1091-1102.e4.
34. Hou J, Jeon B, Baek J, Yun Y, Kim D, Chang B, Kim S, Kim S (2022) High fat diet-induced brain damaging effects through autophagy-mediated senescence, inflammation and apoptosis mitigated by ginsenoside F1-enhanced mixture. J Ginseng Res 46:79-90.
35. Branch SY, Chen C, Sharma R, Lechleiter JD, Li S, Beckstead MJ (2016) Dopaminergic neurons exhibit an age-dependent decline in electrophysiological parameters in the MitoPark mouse model of Parkinson's disease. J Neurosci 36:4026-4037.
36. Hörtnagl H, Tasan RO, Wieselthaler A, Kirchmair E, Sieghart W, Sperk G (2013) Patterns of mRNA and protein expression for 12 GABAA receptor subunits in the mouse brain. Neuroscience 236:345-372.
37. Bäckberg M, Ultenius C, Fritschy JM, Meister B (2004) Cellular localization of GABA receptor alpha subunit immunoreactivity in the rat hypothalamus: relationship with neurones containing orexigenic or anorexigenic peptides. J Neuroendocrinol 16:589-604.
38. Kersanté F, Rowley SC, Pavlov I, Gutièrrez-Mecinas M, Semyanov A, Reul JM, Walker MC, Linthorst AC (2013) A functional role for both -aminobutyric acid (GABA) transporter-1 and GABA transporter-3 in the modulation of extracellular GABA and GABAergic tonic conductances in the rat hippocampus. J Physiol 591:2429-2441.
39. Borden LA, Smith KE, Vaysse PJ, Gustafson EL, Weinshank RL, Branchek TA (1995) Re-evaluation of GABA transport in neuronal and glial cell cultures: correlation of pharmacology and mRNA localization. Recept Channels 3:129-146.
40. Borden LA, Dhar TG, Smith KE, Branchek TA, Gluchowski C, Weinshank RL (1994) Cloning of the human homologue of the GABA transporter GAT-3 and identification of a novel inhibitor with selectivity for this site. Recept Channels 2:207-213.
41. Korgan AC, Wei W, Martin SLA, Kaczorowski CC, O'Connell KMS (2021) High-fat diet induced loss of GABAergic inhibition decouples intrinsic and synaptic excitability in AgRP neurons. bioRxiv. doi: 10.1101/2021.05.31.446473.
42. Ben-Ari Y (2002) Excitatory actions of gaba during development: the nature of the nurture. Nat Rev Neurosci 3:728-739.